Hadronic resonance production with ALICE at the LHC

Sergey Kiselev* for the ALICE Collaboration

*NRC "Kurchatov institute", Moscow, Russia

E-mail: Sergey.Kiselev@cern.ch

Abstract. Recent results on short-lived hadronic resonances obtained with the ALICE detector at LHC energies are presented. These results include system-size and collision-energy evolution of transverse momentum spectra, yields and the ratios of resonance yields to those of longer-lived particles, and nuclear modification factors. Results will be compared with model predictions.

The study of resonance production is important in proton-proton, proton-nucleus, and heavy-ion collisions. Since lifetimes of short-lived resonances are comparable with the lifetime of the late hadronic phase produced in heavy-ion collisions, resonance yields are affected by the regeneration and rescattering of their decay daughters in the hadronic phase. These competing effects are investigated by measuring the yield ratios of resonances to that of the ground state longer-lived hadron as a function of charged-particle multiplicity. From these measurements, it is possible to obtain information on the time interval between the chemical and the kinetic freeze-out. Measurements in pp and p-Pb collisions constitute a reference for nuclear collisions and provide information for tuning event generators inspired by the Quantum Chromodynamics. Moreover, some heavy-ion effects (elliptic flow [1], strangeness enhancement [2], ...) were also unexpectedly observed in small collision systems.

Results on short-lived mesonic $\rho(770)^0$, $K^*(892)^0$, $K^*(892)^{\pm}$, $f_0(980)$, $\phi(1020)$ as well as baryonic $\Sigma(1385)^{\pm}$, $\Lambda(1520)$ and $\Xi(1530)^0$ resonances (hereafter ρ^0 , K^{*0} , $K^{*\pm}$, f_0 , ϕ , $\Sigma^{*\pm}$, Λ^* , Ξ^{*0}) have been obtained using data reconstructed with the ALICE detector. The resonances are reconstructed in their hadronic decay channels and have very different lifetimes as shown in Table 1. The V0A and V0C detectors (32 scintillating counters each) were used for the

Table 1. Reconstructed decay mode, lifetime values [3] and the corresponding references where ALICE results for the hadronic resonances are reported.

	$ ho^0$	K*0	K*±	f_0	$\Sigma^{*\pm}$	Λ^*	Ξ*0	ϕ
decay channel lifetime (fm/c) ALICE papers	$\pi\pi$ 1.3 [4]	Kπ 4.2 [5]-[17]	$K_{\rm S}^0\pi$ 4.2 [19]-[20]	$\pi\pi$ ~ 5 [21]-[22]	$\Lambda \pi$ 5-5.5 [23]-[26]	pK 12.6 [27]-[28]	$\Xi\pi$ 21.7 [23]-[25]	KK 46.2 [5]-[16],[18]

determination of the multiplicity classes by measuring the sum of the signals from V0A and V0C forming the V0M signal.

This contribution reports recent results obtained for K*0 in Xe–Xe at $\sqrt{s_{\rm NN}}$ =5.44 TeV and in pp at 5.02 TeV [17], for K*± in pp at 13 TeV and Pb–Pb at 5.02 TeV [20], for f_0 in p–Pb at 5.02 TeV [22], for $\Sigma^{*\pm}$ and Ξ^{*0} in pp at 13 TeV [25].

Figure 1 shows the transverse momentum spectra of Ξ^{*0} in pp collisions at $\sqrt{s} = 13$ TeV and f_0 in p-Pb collisions at $\sqrt{s_{\rm NN}} = 5.02$ TeV for different multiplicity classes. For $p_{\rm T} < 4$ GeV/c,

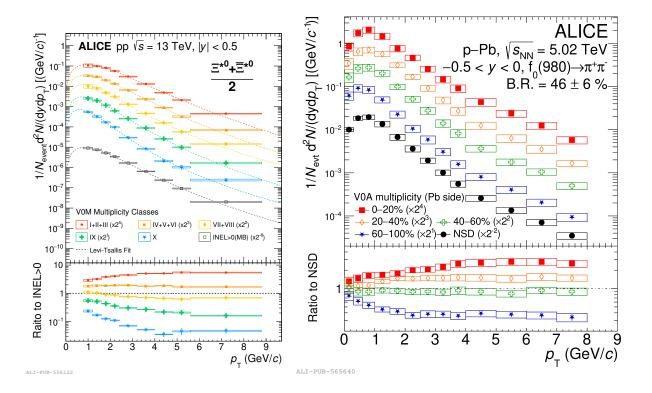


Figure 1. (color online) Transverse momentum spectra of Ξ^{*0} in pp collisions at $\sqrt{s} = 13$ TeV (left) and f_0 in p-Pb collisions at $\sqrt{s_{\rm NN}} = 5.02$ TeV (right) for different multiplicity classes.

a hardening of the $p_{\rm T}$ spectrum from low- to high-multiplicity events is clearly seen, while the spectral shapes in the different multiplicity classes are found to become consistent among each other for $p_{\rm T} > 4~{\rm GeV}/c$. Such trends are similar to those observed for other hadron species [29].

Figure 2 presents the $\mathrm{d}N/\mathrm{d}y$ and $\langle p_\mathrm{T}\rangle$ of K*0 as a function of the charged-particle multiplicity density. For the $\mathrm{d}N/\mathrm{d}y$ new data for pp at $\sqrt{s}=5.02$ TeV and Xe–Xe at $\sqrt{s_\mathrm{NN}}=5.44$ TeV follow a general trend: yields are independent of collision system and appear to be driven by the event multiplicity. The $\langle p_\mathrm{T}\rangle$ rises faster with multiplicity in pp and p–Pb collisions than in Xe–Xe and Pb–Pb collisions. An analogous behavior has been observed in [30] for charged particles and can be understood as the effect of color reconnection between strings produced in multi-parton interactions.

Figure 3 (left) shows the particle yield ratio K^{*0}/K as a function of the charged-particle multiplicity density. The yield ratio in different collision systems shows a smooth evolution with multiplicity, and is independent of the collision system. Observed decrease in the ratio can be understood as the rescattering of K^{*0} meson's decay daughters inside the hadronic phase [10]. Data are compared with EPOS3 [31], γ_S -CSM [32] and HRG-PCE [33] predictions: HRG-PCE gives the best agreement with the data, EPOS3 with the UrQMD afterburner qualitatively

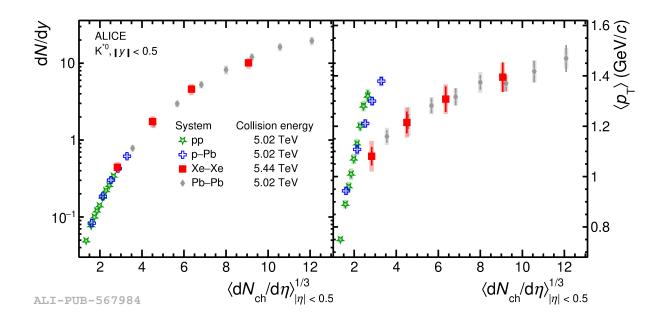


Figure 2. (color online) The $\mathrm{d}N/\mathrm{d}y$ (left) and $\langle p_{\mathrm{T}} \rangle$ (right) of K*0 as a function of the charged-particle multiplicity density in pp collisions at $\sqrt{s} = 5.02$ TeV and Xe–Xe collisions at $\sqrt{s_{\mathrm{NN}}} = 5.44$ TeV. Measurements are compared with the results obtained in p–Pb [7] and Pb–Pb [14] collisions at $\sqrt{s_{\mathrm{NN}}} = 5.02$ TeV.

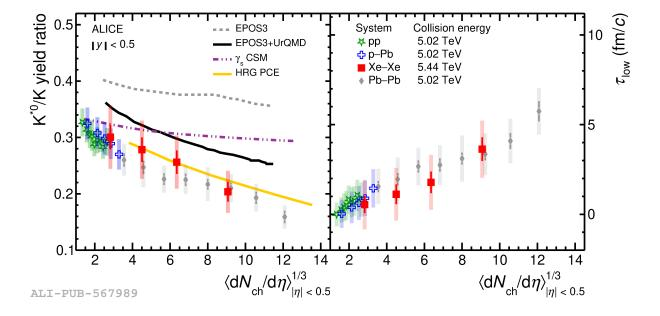


Figure 3. (color online) The particle yield ratio K^{*0}/K (left) and the lower limit of hadronic phase lifetime (right) as a function of the charged-particle multiplicity density in pp collisions at $\sqrt{s} = 5.02$ TeV and Xe–Xe collisions at $\sqrt{s_{\rm NN}} = 5.44$ TeV. Measurements are compared with the results obtained in p–Pb [7] and Pb–Pb [14] collisions at $\sqrt{s_{\rm NN}} = 5.02$ TeV. For the ratio model predictions from EPOS3 [31] with and without the UrQMD afterburner, γ_S -CSM [32] and HRG-PCE [33] are also shown.

reproduces the multiplicity dependence, γ_S -CSM (rescattering effect is not implemented) does not explain the multiplicity dependence. Using the measured ratios and the assumption that there is no regeneration of K*0 in the hadronic medium, one can obtain an estimate of the lower bound of the hadronic phase lifetime τ_{low} , i.e., the time between chemical and kinetic freeze-out, Fig. 3 (right). The τ_{low} smoothly increases with multiplicity and reaches $\sim 5 \text{ fm/}c$.

Figure 4 (left) shows the the multiplicity dependence of the $K^{*\pm}/K$ ratio in pp collisions at $\sqrt{s} = 13$ TeV, compared to the K^{*0}/K one. The decreasing trend already outlined by the K^{*0}

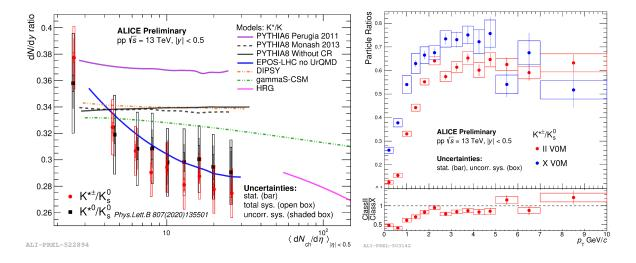


Figure 4. (color online) Left: Ratios $K^{*\pm}/K$ and K^{*0}/K [11] as a function of the charged-particle multiplicity density in pp collisions at $\sqrt{s}=13$ TeV. Model predictions from PYTHIA6 [34], PYTHIA8 [35], EPOS-LHC [36], DIPSY [37], γ_S -CSM (gammaS-CSM) [32] and HRG [33] are also shown. Right: Ratios $K^{*\pm}/K$ as a p_T function for low (X) and high (II) multiplicity classes.

analysis is confirmed by the K* $^{\pm}$ results. The K* $^{\pm}/$ K ratio in the highest multiplicity class is below the low multiplicity value at $\sim 7\sigma$ level taking into account the multiplicity uncorrelated uncertainties ($\sim 2\sigma$ level for the K* $^{0}/$ K ratio). This result represents the first evidence of a clear K*/K suppression measured in small collision systems. EPOS-LHC [36] provides good agreement with the measured data, well reproducing the decreasing trend, while PYTHIA6 [34], PYTHIA8 [35], DIPSY [37] and γ_{S} -CSM tend to overestimate the ratios at high multiplicities and exhibit a fairly flat trend. The ratio of the high multiplicity K* $^{\pm}/$ K differential p_{T} distribution to the low multiplicity one helps to quantify the observed decrease in the particle ratios, Fig. 4 (right). For $p_{T} \leq 2$ GeV/c the double K* $^{\pm}/$ K ratio deviates from unity by more than 3σ suggesting a low p_{T} dominant process.

Ratios $\Sigma^{*\pm}/\Lambda$ (left) and Ξ^{*0}/Ξ (right) are illustrated in Fig. 5. In the new results for pp collisions at $\sqrt{s}=13$ TeV there is a hint of increase of the ratio with increasing multiplicity. Despite similar lifetimes, K^* and $\Sigma^{*\pm}$ exhibit different trends. One of decay daughters $(\Sigma^{*\pm} \to \Lambda \pi, \Xi^{*0} \to \Xi \pi)$ are long-lived particles Λ and Ξ , which decay out of the hadron phase. Only π can be rescattered and the effect of regeneration $\Lambda \pi \to \Sigma^{*\pm}$ can be more pronounced. For the longer-lived Ξ^{*0} , $c\tau$ =21.7, the hadronic stage effects are less important. The EPOS-LHC and PYTHIA8 with Rope shoving predict a slight increase of the ratios.

Figure 6 shows ratios $\Sigma^{*\pm}/\pi$ (left) and Ξ^{*0}/π (right). The results show a smooth increasing trend as a function of multiplicity without energy and collision system dependence. The increase depends on the strangeness content of the resonance; with $\Sigma^{*\pm}$ having a strangeness content (S)

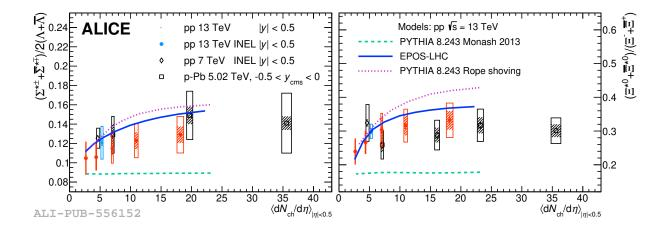


Figure 5. (color online) Ratios $\Sigma^{*\pm}/\Lambda$ (left) and Ξ^{*0}/Ξ (right) as a function of the charged-particle multiplicity density in pp collisions at $\sqrt{s}=13$ TeV. Measurements are compared with the results obtained in pp at $\sqrt{s}=7$ TeV [23] and p–Pb at $\sqrt{s_{\rm NN}}=5.02$ TeV [24]. Model predictions from EPOS-LHC [36], PYTHIA8 [35] and PYTHIA8 with Rope shoving [38] are also shown.

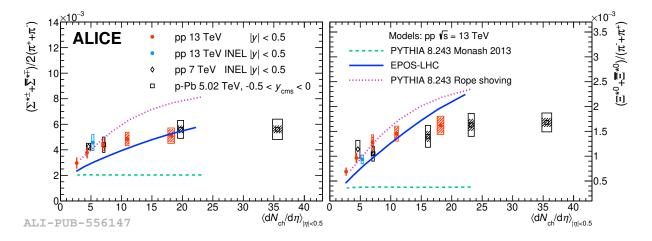


Figure 6. (color online) Ratios $\Sigma^{*\pm}/\pi$ (left) and Ξ^{*0}/π (right) as a function of the charged-particle multiplicity density in pp collisions at $\sqrt{s}=13$ TeV. Measurements are compared with the results obtained in pp at $\sqrt{s}=7$ TeV [23] and p–Pb at $\sqrt{s_{\rm NN}}=5.02$ TeV [24]. Model predictions from EPOS-LHC [36], PYTHIA8 [35] and PYTHIA8 with Rope shoving [38] are also shown.

of 1 and Ξ^{*0} having S=2. These results are consistent with previous measurements of ground-state hyperons to pion ratios with ALICE [39]. EPOS-LHC and PYTHIA8 with Rope shoving predict an increasing trend with multiplicity for both resonances.

To investigate the structure of f_0 , the new ALICE measurements of the f_0 yields are compared to those of other hadrons and resonances with similar mass. Figure 7 (left) shows the double ratio of particle yields to pion yields as a function of multiplicity in p-Pb collisions at $\sqrt{s_{\rm NN}} = 5.02$ TeV. Strangeness enhancement with multiplicity could explain the increase with multiplicity of the ϕ/π ratios. The K^{*0}/π ratios demonstrate the competition between strangeness enhancement and rescattering effect. The f_0/π suppression shows that rescattering

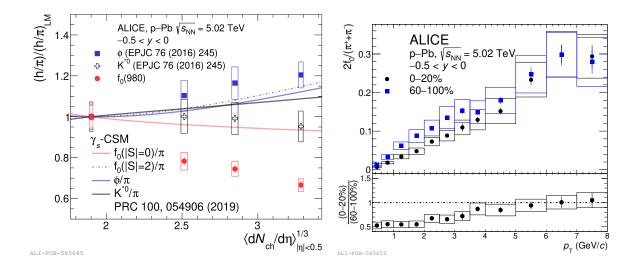


Figure 7. (color online) Left: Double ratio of particle yields to pion yields as a function of multiplicity in p-Pb collisions at $\sqrt{s_{\rm NN}} = 5.02$ TeV. Model predictions from γ_S -CSM [32] are also shown. Right: $p_{\rm T}$ -differential particle yield ratio of f_0 to pion.

is the effect that dominantly affects the yield at low $p_{\rm T}$, Fig. 7 (right). The $p_{\rm T}$ -differential f_0/π ratio does not exhibit the characteristic enhancement of baryon-to-meson ratios, suggesting a structure with two constituent quarks for the f_0 resonance. The γ_S -CSM model qualitatively reproduces the ϕ/π ratio and overestimates the K^{*0}/π ratio. For the f_0/π ratio predictions with zero hidden strangeness, |S|=0, are closer to the data values.

Figure 8 shows the nuclear modification factor $Q_{\rm pPb}$ of f_0 as a function of $p_{\rm T}$ in p–Pb collisions at $\sqrt{s_{\rm NN}}=5.02$ TeV for different multiplicity classes. The $Q_{\rm pPb}$ of f_0 does not exhibit a Cronin-like enhancement. Since baryons demonstrate a Cronin-like enhancement and mesons show little or no nuclear modification [15], [41] might suggest that the f_0 is composed of two quarks. At low $p_{\rm T}<4~{\rm GeV}/c$ the suppression of f_0 becomes more pronounced with increasing multiplicity. This can be explained by the rescattering and radial flow effects.

In summary, recent results on short-lived hadronic resonances obtained by the ALICE experiment in pp, p-Pb, Xe-Xe and Pb-Pb collisions at the LHC energies have been presented. Yields of K^{*0} are independent of the collision system and appear to be driven by the event multiplicity. In pp and p-Pb collisions the $\langle p_{\rm T} \rangle$ values of K^{*0} rise faster with multiplicity than in Xe–Xe and Pb–Pb collisions. One possible explanation could be the effect of color reconnection between strings produced in multi-parton interactions. The K^{*0}/K ratio in different collision systems shows a smooth evolution with multiplicity, and is independent of the collision system. Observed decrease in the ratio can be understood as the rescattering of K*0 meson's decay daughters inside the hadronic phase. Among the models, HRG-PCE gives the best agreement with the data. The lower bound of the hadronic phase lifetime estimated with these ratios smoothly increases with multiplicity and reaches ~ 5 fm/c at highest multiplicity. For pp collisions at $\sqrt{s} = 13$ TeV the K* \pm /K ratio in the highest multiplicity class is below the low multiplicity value at $\sim 7\sigma$ level representing the first evidence of a K*/K suppression measured in pp collisions. The EPOS-LHC model provides good agreement with the measured data. For pp collisions at $\sqrt{s} = 13$ TeV there is also a hint of increase of the $\Sigma^{*\pm}/\Lambda$ and Ξ^{*0}/Ξ ratios with increasing multiplicity. For $\Sigma^{*\pm}$ this may be an indication of the predominance of regeneration over rescattering. The EPOS-LHC and PYTHIA8 with Rope shoving predict a slight increase of the ratios. The $\Sigma^{*\pm}/\pi$ and Ξ^{*0}/π ratios show a smooth increasing trend

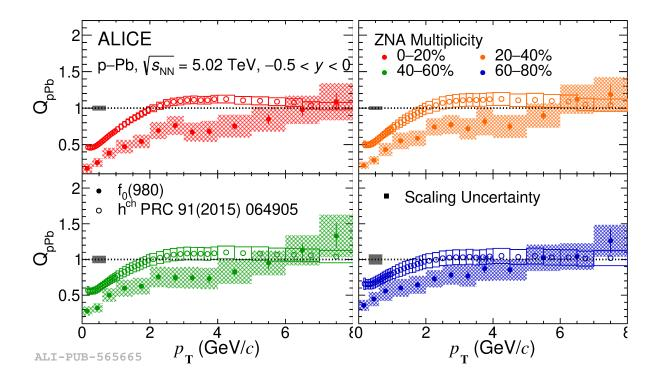


Figure 8. (color online) The nuclear modification factor $Q_{\rm pPb}$ of f_0 as a function of $p_{\rm T}$ in p-Pb collisions at $\sqrt{s_{\rm NN}}=5.02$ TeV for different multiplicity classes. The $Q_{\rm pPb}$ of charged hadrons [40] are reported for comparison.

as a function of multiplicity and are consistent with previous measurements of ground-state hyperons to pion ratios. EPOS-LHC and PYTHIA 8 with Rope shoving predict an increasing trend with multiplicity for both resonances. In p–Pb collisions at $\sqrt{s_{\rm NN}}=5.02$ TeV the f_0/π suppression shows that rescattering is the effect that dominantly affects the yield at low $p_{\rm T}$. The $p_{\rm T}$ -differential f_0/π ratio does not exhibit the characteristic enhancement of baryon-to-meson ratios, suggesting a structure with two constituent quarks for the f_0 resonance. The nuclear modification factor $Q_{\rm pPb}$ of f_0 does not exhibit a Cronin-like enhancement suggesting that the f_0 is composed of two quarks.

The work was carried out within the state assignment of NRC "Kurchatov institute".

References

- [1] Acharya S et al. (ALICE Collaboration) 2019 Phys. Rev. Lett. 123 142301
- [2] Adam J et al. (ALICE Collaboration) 2013 Nature Phys. 13 535
- [3] Workman R L et al. (Particle Data Group) 2022 Prog. Theor. Exp. Phys. 2022 083C01
- [4] Acharva S et al. (ALICE Collaboration) 2019 Phys. Rev. C 99 064901
- [5] Abelev B et al. (ALICE Collaboration) 2012 Eur. Phys. J. C 72 2183
- [6] Abelev B et al. (ALICE Collaboration) 2015 Phys. Rev. C 91 024609
- [7] Adam J et al. (ALICE Collaboration) 2016 Eur. Phys. J. C 76 245
- [8] Adam J et al. (ALICE Collaboration) 2017 Phys. Rev. C 95 064606
- [9] Acharya S et al. (ALICE Collaboration) 2019 Phys. Rev. C 99 024906
- [10] Acharya S et al. (ALICE Collaboration) 2020 Phys. Lett. B 802 135225
- [11] Acharya S et al. (ALICE Collaboration) 2020 Phys. Lett. B 807 135501
- [12] Acharya S et al. (ALICE Collaboration) 2020 Phys. Rev. C **102** 024912
- [13] Abelev B et al. (ALICE Collaboration) 2021 Eur. Phys. J. C 81 256
- [14] Acharya S et al. (ALICE Collaboration) 2022 Phys. Rev. C 106 034907

- [15] Acharya S et al. (ALICE Collaboration) 2023 Phys. Rev. C 107 055201
- [16] Acharya S et al. (ALICE Collaboration) 2023 Eur. Phys. J. C 83 540
- [17] Acharya S et al. (ALICE Collaboration) 2024 Phys. Rev. C 109 014911
- [18] Acharya S et al. (ALICE Collaboration) 2021 Eur. Phys. J. C 81 584
- [19] Acharya S et al. (ALICE Collaboration) 2022 Phys. Lett. B 828 137013
- [20] Acharya S et al. (ALICE Collaboration) 2024 Phys. Rev. C 109 044902
- [21] Acharya S et al. (ALICE Collaboration) 2023 Phys. Lett. B 846 137644
- [22] Acharya S et al. (ALICE Collaboration) 2024 Phys. Lett. B 853 138665
- [23] Abelev B et al. (ALICE Collaboration) 2015 Eur. Phys. J. C 75 1
- [24] Adamova D et al. (ALICE Collaboration) 2017 Eur. Phys. J. C 77 389
- [25] Acharya S et al. (ALICE Collaboration) 2024 J. High Energy Phys. 5 317
- [26] Acharya S et al. (ALICE Collaboration) 2023 Eur. Phys. J. C 83 351
- [27] Acharya S et al. (ALICE Collaboration) 2019 Phys. Rev. C 99 024905
- [28] Acharya S et al. (ALICE Collaboration) 2020 Eur. Phys. J. C 80 160
- [29] Acharya S et al. (ALICE Collaboration) 2020 Eur. Phys. J. C 80 693
- [30] Abelev B et al. (ALICE Collaboration) 2013 Phys. Lett. B 727 371
- [31] Knospe A G et al. 2016 Phys. Rev. C 93 014911
- [32] Vovchenko V, Donigus B, and Stoecker H 2019 Phys. Rev. C 100 054906
- [33] Motornenko A et al. 2020 Phys. Rev. C 102 024909
- [34] Skands P Z 2010 Phys. Rev. D 82 074018
- [35] Skands P Z et al. 2014 Eur. Phys. J. C 74 3024
- [36] Pierog T. et al. 2016 Phys. Rev. C 92 034906
- [37] Flensburg C et al. 2011 J. High Energy Phys. 8 103
- [38] Bierlich C, Gustafson G, and Lönnblad L 2018 Phys. Lett. B 779 58
- [39] Acharya S et al. (ALICE Collaboration) 2020 Eur. Phys. J. C 80 167
- [40] Adam J et al. (ALICE Collaboration) 2015 Phys. Rev. C 91 064905
- [41] Adam J et al. (ALICE Collaboration) 2016 Phys. Lett. B 760 729